ELSEVIER

Ceramics International 25 (1999) 479–483

CERAMICS INTERNATIONAL

Study on crystallization kinetics of plasma sprayed hydroxyapatite coating

Chengkang Chang*, Jingqi Huang, Jiyu Xia, Chuanxian Ding

Shanghai Institute of Ceramics, Chinese Academy of Sciences, Shanghai 200050, People's Republic of China

Received 9 March 1998; accepted 8 July 1998

Abstract

Hydroxyapatite (HAp) coatings were deposited using vacuum plasma spraying system. Peak intensities of lattice plane (211), (112), (300) in XRD patterns were employed to investigate crystallinities of as-received coatings. Heat treatments at temperatures 600, 650, 700 and 800°C were proceeded to reveal crystallization kinetics of vacuum plasma sprayed hydroxyapatite coating. Computer software was used to deal with the data processing. The results obtained showed that, after vacuum plasma spraying, crystallinity of hydroxyapatite coating decreases greatly, implying that the as-received coating mainly consists of an amorphous phase. Heat treatment is effective for the amorphous phase to convert into crystalline in vacuum plasma sprayed hydroxyapatite coating depending on heat treatment time and temperature. The conversion of hydroxyapatite from amorphous to crystalline is a second order reaction, and the activation energy is calculated to be 11.31×10^4 kJ/mol.

1. Introduction

Hydroxyapatite had been confirmed to be bioactive since it was first made in the 1970's. The artificial synthetic material had been used as an important biomaterial for numerous medical applications, such as orthopaedical and dental implants [1,2]. Having the similar composition and crystal structure to the apatite in living bone, it has excellent osteoconductive and bioactive properties, which could induce bone formation along its surface and form strong biological fixation [3,4]. It could bond to bone tissues directly without bone resorption around it. The main problem preventing the material from being widely used in medicine is its poor mechanical properties. The brittleness of the ceramics makes them incapable of being used in load bearing situations [5,6]. Recently, new developments in surface technology are creating new ways and possibilities of incorporating hydroxyapatite to be used in conjunction with mechanically strong metallic substrates to enhance osseointegration.

Up until now, many methods had been tried to apply hydroxyapatite onto metallic substrates, including sol-gel methods, chemical deposition, ion-sputtering deposition, thermal spraying and so on [7–10]. Among the methods used, the most widely employed is the plasma spraying technique. Since 1985, implants with plasma sprayed hydroxyapatite coating were used clinically a great deal. Many investigations about in vitro and in vivo behavior of hydroxyapatite coatings were published in the literature, showing the different dissolution of coatings from that of bulk hydroxyapatite ceramics. This is ascribed to the plasma spraying induced phase changes of hydroxyapatite.

A recent study on coating manufacturing done by J. Weng et al., showed that, during the plasma spraying process, hydroxyapatite particles were melted to droplets and rapidly re-solidified on the substrate to form splats. In the process, amorphorization and decomposition of apatite in the coating took place [11,12]. Crystallinity of starting powder and surface temperature of substrate were regarded as two important factors which affect the coating crystallinity [13–15]. Post heat treatment and water vapor treatment were proved to be effective ways to convert amorphous hydroxyapatite into crystalline [16–18].

In the current study, hydroxyapatite coatings were prepared using a vacuum plasma spraying system. Post heat treatment of temperature from 600 up to 800°C was applied to the as-received coatings to investigate the crystallization kinetics of hydroxyapatite coating.

* Corresponding author. E-mail:ckchang@mail1.stju.edu.cn

0272-8842/99/$20.00
PII: S0272-8842(98)00063-7

2. Experimental procedure

The raw material used in the study was supplied by Sulzer Metco, Switzerland. with particle size from 45 to 180 μm and a mean size of 100 μm. Chemical analysis supplied by the manufacturer showed that the powder was of high purity, with the harmful impurity being: As (< 0.5 μg/g), Cd (< 0.2 μg/g), Pb (< 1 μ g/g), and Hg (< 0.5 μ g/g). The substrate, Ti6A14V alloy, was shaped into a dimension of 20×10×4 mm, sand blasted by alumina sand with an average surface roughness of 20μm. Vacuum plasma spraying was carried out using a vacuum plasma spraying system from Switzerland, under the general condition listed in Table 1. Heat treatment was made under temperature of 600, 650, 700 and 800°C, with a time ranging from 0.5 to 8 h. Phase analyses of as-received coatings were conducted using an X-ray diffractometer at 40 kv and 100 mA. Scans were run from 20 to 70°, with a 2θ step of 0.02° and a time increment of 3 s. Copper k_a X-rays of wavelength 1.5418 A were generated. Crystallinities of all samples were calculated from the XRD patterns using the peak intensities of the three strongest lines of hydroxyapatite. A standard curve for calculation of crystallinity was made from the XRD patterns of hydroxyapatite powders mixed with a specially made amorphous bioglass with hydroxyapatite content of 10, 30, 50, 70 and 90 wt%.

3. Results and discussion

3.1. Standard curve for calculating crystallinities of hydroxyapatite coating

XRD patterns of powder with hydroxyapatite content from 10 to 90 wt% were shown in Fig. 1. It can be seen from the patterns that all the peak intensities decreased with the decrease in hydroxyapatite content of tested powders. Furthermore, bulges around 25–35° 2θ degree became more and more obvious showing an increment in the amorphous phase. Table 2 lists the exact peak intensities of the three strongest lines of lattice plane (211), (112) and (300). Samples 1–5 represent tested samples with hydroxyapatite content of 10, 30, 50, 70 and 90 wt%. The intensities of bioglass were cut off from the XRD pattern.

Fig. 2 revealed the relationship between peak intensity and hydroxyapatite content. From Fig. 2, it can be seen that, the data of the three different lattice planes

Table 1
Vacuum plasma spraying parameters plasma spraying parameters

Plasma spraying parameters	
Primary plasma gas	Ar, 50 s1pm
Secondary plasma gas	H_2, 10 s1pm
Carrier gas	Ar, 1.5 s1pm
Powder flow rate	20 g/min
Plasma jet type	F4-VB
Injector	Φ 1.8 mm
Chamber pressure	150 mbar
Spray power	30–45 kw
Spray distance	275 mm
Thickness of coating controlled	100 μm

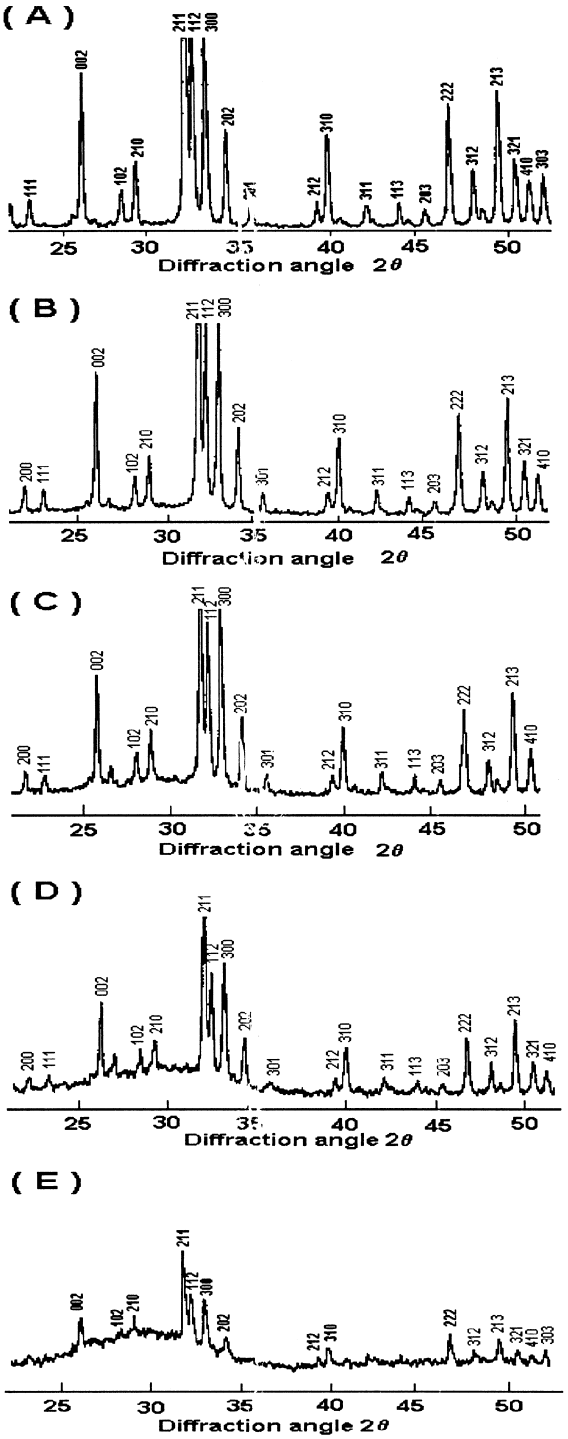

Fig. 1. XRD patterns of samples with different hydroxyapatite contents: (A): 90wt%; (B) 70wt%; (c) 50wt%; (D) 30wt%; (E) 10wt%.

Table 2
Peak intensities of lattice plane (211), (112),(300) obtained from XRD patterns

	Peak intensities of samples with different hydroxyapatite content (cps)				
	Sample 1	Sample 2	Sample 3	Sample 4	Sample 5
Lattice plane (211)	556	1427	2692	3533	4300
Lattice plane (112)	297	749	1208	1600	2160
Lattice plane (300)	305	842	1513	2120	2630

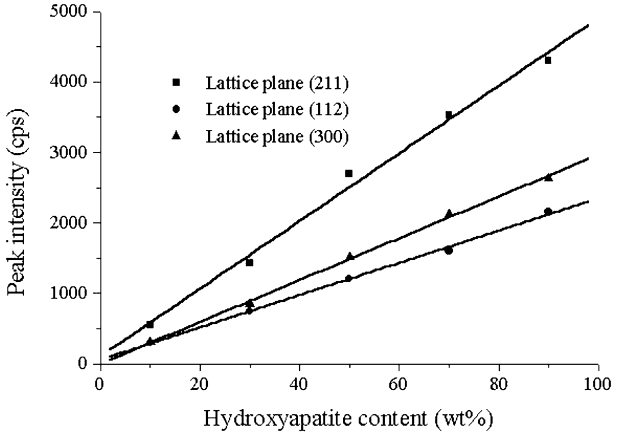

Fig. 2. Standard curve for calculating crystallinities of as-received hydroxyapatite coatings. Lattice plane (112), (211) and (300) are the three strongest lines in JCPDS card 09-432.

showed a linear relationship. Computer software, ORIGIN 4.0 was employed to carry out the fitting. The results are listed in Table 3, which indicate that a good linear relationship did exist between diffraction intensity and hydroxyapatite content. Therefore, peak intensity of lattice plane (211) was chosen as a standard to calculate crystallinities of as-received coating. For the vacuum plasma sprayed hydroxyapatite coating, crystallinity calculated according to XRD pattern was 7.8%, implying that the vacuum sprayed coating mainly consists of an amorphous phase. Fig. 3 gives the crystallinities of heat treated coatings. The values varied from 7.8 to 90% depending on heat treatment condition. It can be seen from Fig. 3 that, both heat treatment time and temperature had a great effect on the crystallinities of

Table 3
Computer linear fitting results

	Plane (211)	Plane (112)	Plane (300)
Data number	5	5	5
Output equation	I(intensity) = A + B×C(hydroxyapatite content)		
A Value	103.1	58.55	0
B value	47.97	22.89	29.64
Confidence	99.62%	99.87%	99.91

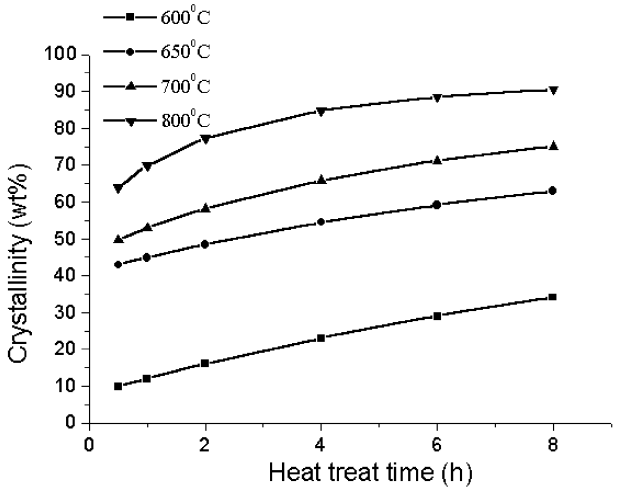

Fig. 3. Crystallinities of coatings heat-treated under different temperature with time from 0.5 to 8 h.

heat-treated hydroxyapatite coatings. At the beginning, the conversion of hydroxyapatite from amorphous to crystalline went quickly. As time went on, the conversion rate reduced gradually. The final crystallinity of HA coatings heat treated for 8 h under different temperature were quite different, varying from 34% for 600 to 90% for 800°C.

3.2. Crystallization kinetics of plasma sprayed hydroxyapatite coating

According to the theories of chemical reaction kinetics, the conversion of hydroxyapatite from amorphous phase to crystalline should follow Arrhenius formula:

$$\frac{dC_{ACP}}{dt} = kC_{ACP}^{n} \tag{1}$$

$$k = Ae^{-E/RT} \tag{2}$$

$$C_{ACP} = C_{ACP}^{0}(1-\alpha) \tag{3}$$

where C_{ACP} is the content of amorphous hydroxyapatite in heat-treated samples, k is the rate constant, n is the reaction order, E is the activation energy, C_{ACP}^{0} is the initial value of the content of amorphous hydroxyapatite of as-received coating and a is the conversion ratio of hydroxyapatite from amorphous phase to crystalline.

Since the heat treatment procedures were carefully controlled in same condition, Eqs. (1)–(3) can be converted into the following:

$$\frac{d\alpha}{dt} = k'(1-\alpha)^{n} \tag{4}$$

$$k' = A' e^{-E/RT} \tag{5}$$

$$\ln \frac{d\alpha}{dt} = n \ln(1-\alpha) + B \tag{6}$$

where A' and B are constants.

From Eqs. (4)–(6), it can be concluded that, it is the conversion ratio, not the crystallinity that determines the overall conversion kinetics. In Fig. 4, $\ln(d\alpha/dt)$ was plotted against $\ln(1-\alpha)$ using data in Fig. 3. Computer linear fitting revealed a linear relationship. The slopes of four lines represent the reaction order for different temperatures. It was found by the fitting that the reaction order, n, for temperature 600°C is 2.24, 650°C is 1.81, 700°C is 1.86 and 800°C is 2.01. The results indicate that, under different heat treatment temperatures, all the conversion processes from amorphous phase to crystalline follow second order reaction kinetics. Therefore, Eq. (4) can be integrated into following:

$$\frac{1}{1-\alpha} = k't + C \tag{7}$$

where C is the constant of integration.

In Fig. 5, $\frac{1}{1-\alpha}$ was plotted against heat treatment time, the slopes of the four plots were as follows:

600°C, $k'_{600} = 0.05464$,
650°C, $k'_{650} = 0.12716$,
700°C, $k'_{700} = 0.26969$,
800°C, $k'_{800} = 0.99177$.

From Eq. (5), it can be concluded that, when $\ln k'$ is plotted against $1/T$, the slope of the plot should equal to $-E/RT$.

Fig. 6 showed the relationship between $\ln k'$ and $1/T$. Computer linear fitting gives the slope of the plot, which is -13.61×10^3. Therefore, the reaction activation energy, $E = 13.61\times10^3\times8.31 = 11.31\times10^4$kJ/mol.

Therefore, the rate law of the conversion of hydroxyapatite in the vacuum plasma sprayed coating from amorphous phase to crystalline should be:

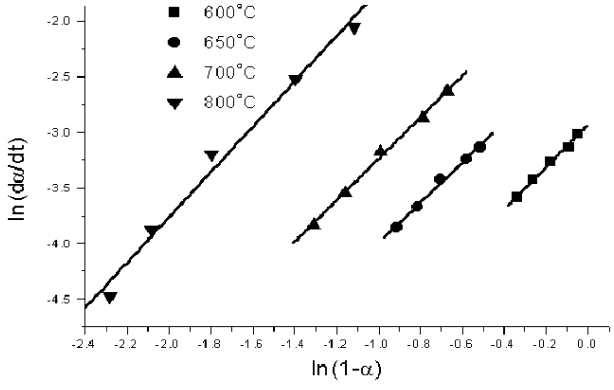

Fig. 4. Plots of $\ln(d\alpha/dt)$ against $\ln(1-\alpha)$ for temperatures 600, 650, 700 and 800°C.

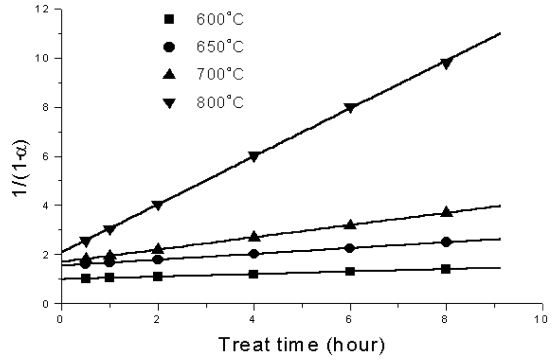

Fig. 5. Plots of $\ln(1-\alpha)$ against heat treatment time.

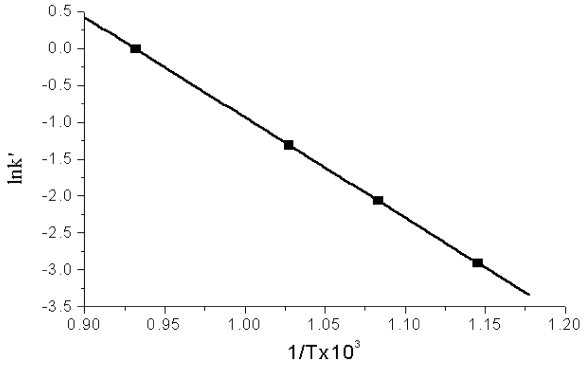

Fig. 6. Plot of $\ln k'$ against $1/T$. The slope of the plot is equal to $-E/RT$.

$$\frac{dC_{ACP}}{dt} = A e^{-E/RT} C_{ACP}^2 \tag{8}$$

4. Conclusion:

In the study, peak intensities of lattice plane (211), (112), (300) were proved by computer linear fitting data as standards for calculating crystallinities of hydroxyapatite coatings. Crystallinity of as-received coating produced by vacuum plasma spraying was 7.8%, which indicated that the coating mainly consists of an amorphous phase. After heat treatment, the amorphous phase in hydroxyapatite coating converted to crystalline. Both heat treatment time and temperature had a great effect on the conversion. Further study showed that, the conversion reaction follows second order chemical reaction kinetics, and the reaction activation energy is 11.31×10^4 kJ/mol.

References

[1] S. Ozawa, S. Kasugai, Evaluation of implant materials (hydroxyapatite, glass-ceramics, titanium) in rat bone marrow stromal cell culture, Biomaterials 17 (1996) 23–29.

[2] V. Passi, V. Tarrible Weil Marin, A. Miotti, A. Pareti, Hydroxyapatite in oral surgery: clinical and histological results, in: P. Vincenzini (Ed.), Ceramics in Substitutive and Reconstructive Surgery, Elsevier science publications, 1991, pp. 467–476.
[3] B.W. Schreurs, R. Huiskes, P. Buma, T.J.H. Slooff, Biomedical and histological evaluation of a hydroxyapatite-coated titanium femoral stem fixed with an intramedullary morsellized bone grafting technique: an animal experiment on goat, Biomaterials 17 (1996) 1176–1186.
[4] J.A. Jansen, J.P.C.M. Van Der Wherden, J.G.C. Wolke, A histological evaluation of the effect of hydroxyapatite coating on interfacial response, Journal of Materials Science:, Materials in Medicine 4 (1993) 466–470.
[5] J. Li, L. Hermansoon, Mechanical evaluation of hot isostatically pressed hydroxyapatite, Interceramics 39 (2) (1990) 13–15.
[6] M. Akao, H. Aoki, K. Kato, Mechanical properties of sintered hydroxyapatite for prosthetic application, Journal of Materials Science 16 (1981) 809–812.
[7] M. Schirkhanzadeh, Electrochemical fabrication of bioactive composite coatings on Ti6A14V surgical alloy, Materials Letters 14 (1992) 27–30.
[8] K.A. Gross, C.C. Bernt, Thermal spraying of hydroxyapatite for bioceramic applications, Key Engineering Materials 53–55 (1991) 124–129.
[9] M. Schirkhanzadeh, Bioactive calcium phosphate coatings prepared by electrodeposition, Journal of Material Science Letter 10 (1991) 1415–1417.
[10] P. Li, K. de Groot, T. Kokubo, Bioactive $Ca_{10}(PO_4)_6(OH)_2$-TiO_2 composite coating prepared by sol-gel process, Journal of Sol-gel Science and Technology 7 (1996) 27–34.
[11] Z. Zyman, J. Weng, X. Liu, X. Zhang, Z. Ma, Amorphous phase and morphological structure of hydroxyapatite plasma coatings, Biomaterials 14 (1993) 225–228.
[12] J. Weng, X. Liu, X. Zhang, X. Ji, Thermal decomposition of hydroxyapatite in coatings influenced by underlying titanium during plasma spraying and post-heat-treatment, Journal of Biomedical Material Research 30 (1996) 6–12.
[13] Weidong. Tong, Jiyong. Chen, Xingdong. Zhang, Amorphorization and recrystallization during plasma spraying of hydroxyapatite, Biomaterials 16 (1995) 829–832.
[14] J. Weng, X. Zhang, Recrystallization of apatite in plasma sprayed coatings, in: O.H. Anderson, A. Yli-Urpo (Eds.), Bioceramics 7, Butterworth-Heinemann Ltd., Cambridge, 1994, pp.235–240.
[15] J. Weng, X. Liu, X. Li, X. Zhang, Intrinsic factors of apatite influencing its amorphization during plasma spray coating, Biomaterials 16 (1995) 39–44.
[16] Z. Zyman, J. Weng, X. Liu, X. Li, X. Zhang, Phase and structure changes in hydroxyapatite coatings under heat treatment, Biomaterials 15 (1994) 151–155.
[17] J. Weng, Y. Cao, J. Chen, X. Zhang, Siginicance of water promoting amorphous to crystalline conversion of apatite in plasma sprayed coatings, Journal of Material Science Letter 15 (1995) 211–213.
[18] Y. Cao, J. Weng, J. Chen, J. Feng, Z. Yang, X. Zhang, Water vapor treated hydroxyapatite coatings after plasma spraying and their characteristics, Biomaterials 17 (1996) 419–424.